

## RESEARCH/REVIEW ARTICLE

# Topography, ice thickness and ice volume of the glacier Pedersenbreen in Svalbard, using GPR and GPS

Songtao Ai,<sup>1</sup> Zemin Wang,<sup>1</sup> Dongchen E,<sup>1</sup> Kim Holmén,<sup>2</sup> Zhi Tan,<sup>1</sup> Chunxia Zhou<sup>1</sup> & Weijun Sun<sup>3</sup><sup>1</sup> Chinese Antarctic Center of Surveying and Mapping, Wuhan University, Wuhan 430079, People's Republic of China<sup>2</sup> Norwegian Polar Institute, Fram Centre, NO-9296 Tromsø, Norway<sup>3</sup> Cold and Arid Regions Environmental and Engineering Research Institute, Chinese Academy of Sciences, Lanzhou 730000, People's Republic of China**Keywords**

GPR; GPS; glacier topography; ice volume; ice thickness; Pedersenbreen.

**Correspondence**Songtao Ai, Chinese Antarctic Center of Surveying and Mapping, Wuhan University, Wuhan 430079, P. R. China.  
E-mail: ast@whu.edu.cn**Abstract**

Pedersenbreen is a small valley glacier (ca. 6 km<sup>2</sup> in 2009), ending on land, located in north-western Spitsbergen, Svalbard. Ground-based radio-echo sounding in April 2009, using a 100-MHz commercial radar and a self-made low-frequency radar, revealed a polythermal structure. The radar was coupled with a global positioning system device to geo-reference the traces. Each radar profile was manually edited to pick the reflection arrival time from the interface between ice and bedrock. Travel times were converted to ice thickness using a velocity of 0.165 m/ns, which was estimated from common mid-point measurement. Then the surface topography, bedrock topography, ice thickness contours and ice volume were derived using interpolation methods. Because it was difficult to distinguish the reflection wave from the background with the 100-MHz radar in some of the thickest areas of Pedersenbreen, we used a 5-MHz radar of our own design to fill in this gap. The maximum thickness of Pedersenbreen reaches  $183 \pm 9$  m, and the ice volume is  $0.393 \pm 0.047$  km<sup>3</sup> in 2009. Comparing these data with the surface topographical data available for 1936 indicates a mass loss of nearly 12% during the past 73 years.

With 60% of its area covered by glaciers and ice caps (Hagen & Liestøl 1990), the archipelago of Svalbard (74–81°N, 10–35°E) is dominated by small polythermal glaciers. Monitoring and studying such glaciers in Svalbard is particularly important since they respond rapidly to climate change and play an important role in sea-level change on decadal to centennial scales (Meier 1984; Oerlemans & Fortuin 1992; Hagen et al. 2003).

Pedersenbreen is a small valley glacier with an area of approximately 6 km<sup>2</sup> located on the peninsula of Brøggerhalvøya, north-western Spitsbergen, Svalbard (Fig. 1). Its neighbouring glaciers, Kronebreen and Kongsvegen, have been extensively studied (e.g., Hagen et al. 2005; Kääb et al. 2005; Rolstad & Norland 2009; Moholdt et al. 2010; Köhler et al. 2012). Pedersenbreen is, in contrast, poorly studied and basic parameters for the glacier are lacking. This paper presents a base study of Pedersenbreen, using information derived from the global positioning system (GPS) and ground-penetrating radar (GPR).

GPR is an efficient tool for detecting the ice thickness of glaciers, buried ice crevasses, water channel locations and the glacier thermal regime (e.g., Macheret & Zhuravlev 1982; Hagen & Sætrang 1991; Hambrey et al. 2005; Rolstad & Norland 2009). We collected more than 45 km of simultaneous GPR and GPS profiles on Pedersenbreen, from which we retrieved the ice thickness and surface elevation and constructed maps of surface and bedrock topography, and estimated the ice volume of Pedersenbreen.

**Data collection****GPS data**

Since July 2004, a GPS tracking station has been set up beside the Chinese Arctic Yellow River Station, in Ny-Ålesund, Spitsbergen, Svalbard. Five observation stakes have been in place along the central line of

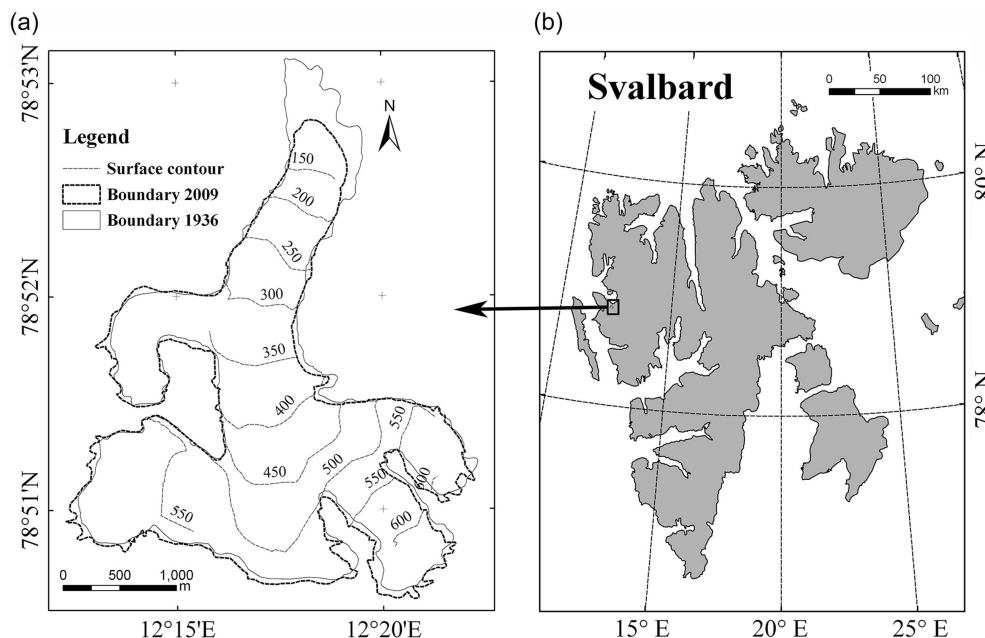


**Fig. 1** (a) Sketch view of Pedersenbreen and (b) map of the main islands of Svalbard indicating the location of Pedersenbreen.

Pedersenbreen since July 2005. The movement of these stakes has been monitored annually with high precision using dual-frequency GPS instruments (Ai et al. 2006; Xu et al. 2010).

During a two-week period in April 2009, high density GPS points were collected on the surface of Pedersenbreen using a Smart-V1 GPS unit (NovAtel, Calgary, AB, Canada). Though the horizontal accuracy claimed by the manufacturer is within 0.2–1.8 m, in practice this level of accuracy is usually difficult to reach, requiring some additional post-processing of the acquired data. Consequently, we reprocessed the GPS data to improve its precision, using the procedure described in the methods section below.

The five observation stakes (Fig. 2b) have also been measured using a dual-frequency GX1230 GPS unit (Leica Geosystems, Heerbrugg, Switzerland) in April 2009. The highly accurate coordinates from the stakes were utilized to verify the altitude data acquired from the Smart-V1 GPS unit.

**GPR profiles**

The main GPR unit used was the pulseEKKO PRO (Sensors & Software, Mississauga, ON, Canada). 100 MHz antennas were chosen to survey on Pedersenbreen also during April 2009. Two antennas were placed horizontally on two all-wood sledges separated by 4 m, and dragged slowly behind a snowmobile so that the two antennas were parallel to each other and perpendicular

to the profiling direction. The integrated GPS was fixed to the first sledge connecting with the GPR receiver (Fig. 2a). The GPR traces with synchronous GPS coordinates were collected at one-second frequency. Each GPR trace had a time window of 2.8  $\mu$ s, which was stacked four times and composed of 3500 samples. In total, 16 400 traces were collected, which summed to 45.7 km of distance (Fig. 2b). It is of high density such that the average distance between two neighbouring traces was about 3 m.

With GPR measurement on glaciers, the absorption and scattering of radio-signals by meltwater, soaked firn and ice lenses increase with radio frequency (Smith & Evans 1972). For most of the 16 400 traces, the transmitted and reflected signals were clearly presented. A minority of the traces—all acquired over the deepest central cirque area—displayed weak reflected signals. So, a low-frequency (5-MHz) radar (Fig. 2c) of our own design was used to collect a few traces along the central flowline of the glacier. These traces were used to verify the depth from high density traces and fill in for missed bed-echoes by the 100 MHz radar.

**Radio wave velocity validation**

Polar ice typically has a radio-wave velocity (RWV) of 0.168 m/ns (Paterson 1981). But different glaciers have different temperatures and structures, which results in variable velocities. Two common mid-point (CMP) profiles were measured at the tongue of Pedersenbreen

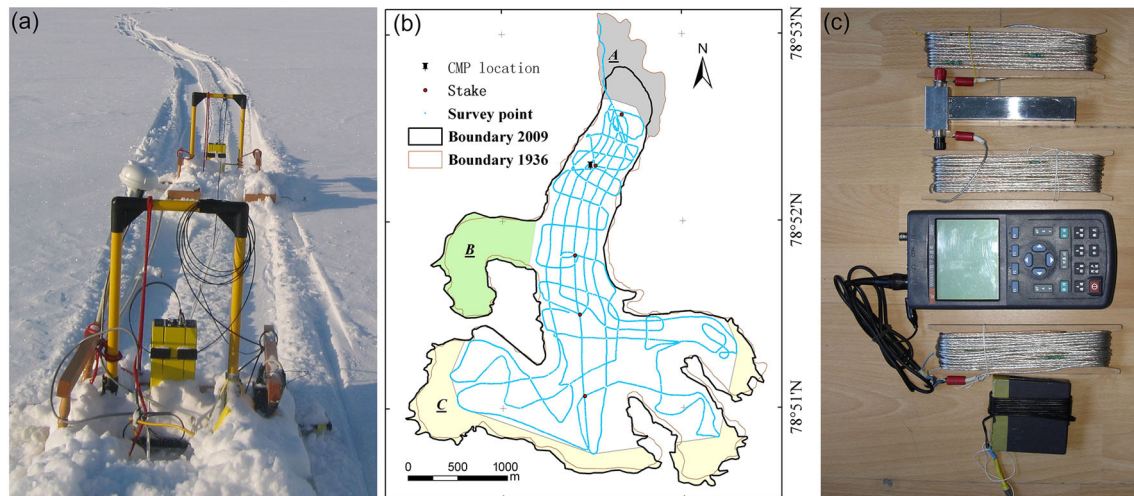


**Fig. 2** (a) The pulseEKKO PRO ground-penetrating radar and global positioning system devices as they were deployed on the glacier Pedersenbreen. (b) The data points of the survey profiles marked on a map with the WGS84 coordinate system. The grey area marked A ( $0.48 \text{ km}^2$  in 1936 and  $0.15 \text{ km}^2$  in 2009) is the part of the tongue that retreated during 1936–2009 and is no longer ice-covered. The green area labelled B ( $0.62 \text{ km}^2$ ) is the north-western tributary of Pedersenbreen, which is inaccessible due to an icefall so there are no survey data for this area. The yellow area marked C ( $1.10 \text{ km}^2$ ) is the high elevation boundary area, covered with thin snow or firn. The boundary lines are from old maps (Norwegian Polar Institute 1990, Norwegian Polar Institute 2008). (c) Self-made low-frequency radar device, whose main parts comprise an oscilloscope (1), transmitter (2), transmitting antenna (3) and receiving antenna (4).

(Fig. 2b). Then, the velocity distribution could be acquired using the CMP analysis function of the EKKOView Deluxe software. We found that the RWV in the upper layer is higher than in the lower layer of Pedersenbreen. This is probably due to the increasing density and the increasing water fraction with increasing depth. Based on these results, an approximate velocity of  $0.165 \text{ m/ns}$  was chosen in this study to process GPR data for Pedersenbreen. We should point out that other authors have used a higher RWV, on the order of  $0.170 \text{ m/ns}$ , for GPR data collected on Svalbard polythermal glaciers during springtime (e.g., Bælum & Benn 2011), which probably implies a relative error in RWV here.

## Methods

Using the GPS points, a digital elevation model (DEM) of the glacier surface was derived after data processing with an interpolation method. The DEM is the basis for our topographical map of the glacier.

## Data analysis

Because the Smart-V1 GPS works at a single frequency, the coordinates acquired directly from the GPS were not of sufficiently high precision. From the cross-over points between tracks, we were able to evaluate the precision of the GPS survey. There are two kinds of cross-over points.

One is the cross-over point between different profiles. The other is the cross-over point within a profile (e.g., a long surveying track turned around and crossed over itself). The statistical data for the height differences are presented in Table 1.

The data in Table 1 indicate that within one profile the height differences were relatively small—root mean square error (RMSE) is only  $0.23 \text{ m}$ —but the height differences between different profiles were much larger, which means that there were systematic errors between different profiles. This was mainly due to variable ionospheric and lower atmospheric conditions as well as satellite distributions between the different profile measurements. To acquire the best possible DEM, the height data needed to be improved by reducing the data error between the different profiles as much as possible; our procedure for doing this is presented below.

The height data from GPS measurements is ellipsoidal height, which needs to be converted into elevation above sea level before further data processing. Fortunately, an elevation benchmark near the glacier ( $< 10 \text{ km}$ ) was found in Ny-Ålesund whose elevation was determined to

**Table 1** Height differences of cross-over points.

Type	Count	Maximum error (m)	Root mean square error (m)
Within same profiles	266	2.78	0.23
Between different profiles	101	−8.2	2.69

13.40 m from one map (Norwegian Polar Institute 1990). Its GPS height was 48.558 m, as determined from GPS measurement in April 2009. The geoidal height at this point was then determined to be 35.158 m, which was subsequently used to convert the measured GPS heights to altitude above sea level.

### Data adjustment

The reasoning that follows is based on the assumption that the altitude correction for a given profile is the same for all of its points; this may not hold true if, for instance, there is a drift with time of the GPS-recorded altitude, something not unusual when using a stand-alone GPS device. Moreover, it is assumed that no data biases are presented.

In order to improve the altitude data quality, a least square method was used to process the GPS data. Assume that each profile needs an altitude corrective variable  $\delta h_j$  ( $j = 1, 2, \dots, n$ ; here  $n$  is the number of profiles). At each crossing GPS point between different profiles, the residual altitude data error  $v_i$  ( $i = 1, 2, \dots, m$ ; here  $m$  is the number of cross-over points) is as in Eqn. 1:

$$v_i = (H_{ik} + \delta h_k) - (H_{il} + \delta h_l); k, l \in \{1, 2, \dots, n\} \quad (1)$$

Here  $H_{ik}$  and  $H_{il}$  are the actual altitude data of the cross-over points in the dependent profile  $k$  and profile  $l$ .  $\delta h_k$  and  $\delta h_l$  are the altitude corrective variables of the dependent profile  $k$  and profile  $l$ .

Then, the least squares method finds its optimum when the sum,  $S$  in Eqn. 2, of squared residuals is a minimum.

$$S = \sum_{i=1}^m v_i^2 \quad (2)$$

At the same time we need a rule, Eqn. 3, to keep the altitude benchmark.

$$\sum_{j=1}^n \delta h_j = 0 \quad (3)$$

Because residual altitude errors remain after the adjustment shown in Eqns. 2 and 3, we smoothed the altitude data around the crossing points using an inverse distance weighted method (Bartier & Keller 1996). The statistical data after this processing are presented in Table 2.

The data in Table 2 show just the internal consistency from GPS survey on April 2009. Compared with the altitude data of the observation stakes from the dual-frequency GPS measurement at coincident points, the accuracy, in absolute value, of the data was calculated to within 0.8 m after smoothing. This data accuracy, which

**Table 2** Altitude differences in different types of crossing profiles.

Type	Maximum error (m)	Root mean square error (m)
Actual data	-8.20	2.69
After adjustment	-4.01	1.35
After smoothing	-0.71	0.29

is less than the seasonal variations in the altitude and the year-round melting, was sufficient for our purposes.

### Surface topography

From the measured points on the glacier, the DEM of the glacier surface can be derived via Kriging interpolation from the adjusted and smoothed point data. As the RMSE values in Table 2 show, the altitude differences between cross-over GPS points produced a rough surface, and the processed data show a much smoother surface.

A contour map (Fig. 3b) was derived from the DEM using ArcMap software. The planar area was calculated to be 4.462 km<sup>2</sup> within the surveyed extent, which excludes three areas without survey, the unsurveyed tongue area (0.15 km<sup>2</sup>), the north-western tributary (0.62 km<sup>2</sup>) and the high elevation uphill boundary areas (1.104 km<sup>2</sup>). So the planar area should be 6.34 ± 0.07 km<sup>2</sup> in total. The error in the planar area was estimated as the product of the glacier perimeter times the uncertainty of 3 m assumed for the positioning of the glacier boundary.

### Bedrock topography and ice volume estimation

In the same way as for the surface DEM, a bedrock DEM was derived using the ice thickness data from GPR combined with the GPS locations. But the depth difference between crossing profiles was much larger than the difference in GPS height. Most depth difference values lie in a Gaussian distribution with RMSE about 4.6 m, with a few values over 15 m. These discrepancies are probably due to misinterpretation during the ice–bedrock interface picking procedure. In contrast, most GPS height difference values lie in a Gaussian distribution with a standard deviation less than 1.5 m after adjustment.

Here we should point out that the 100-MHz radar cannot get a continuously clear reflection signal in the deepest area of the glacier, where temperate ice is probably located (Hagen & Sætrang 1991). So we used the 5-MHz radar of our own design to get some sparse point data, which filled in the data gap. After the data processing for all the traces from GPR survey, a depth distribution map was obtained (Fig. 3a). The bedrock contour map (Fig. 3b) was then obtained by subtracting the thickness data from the surface DEM.

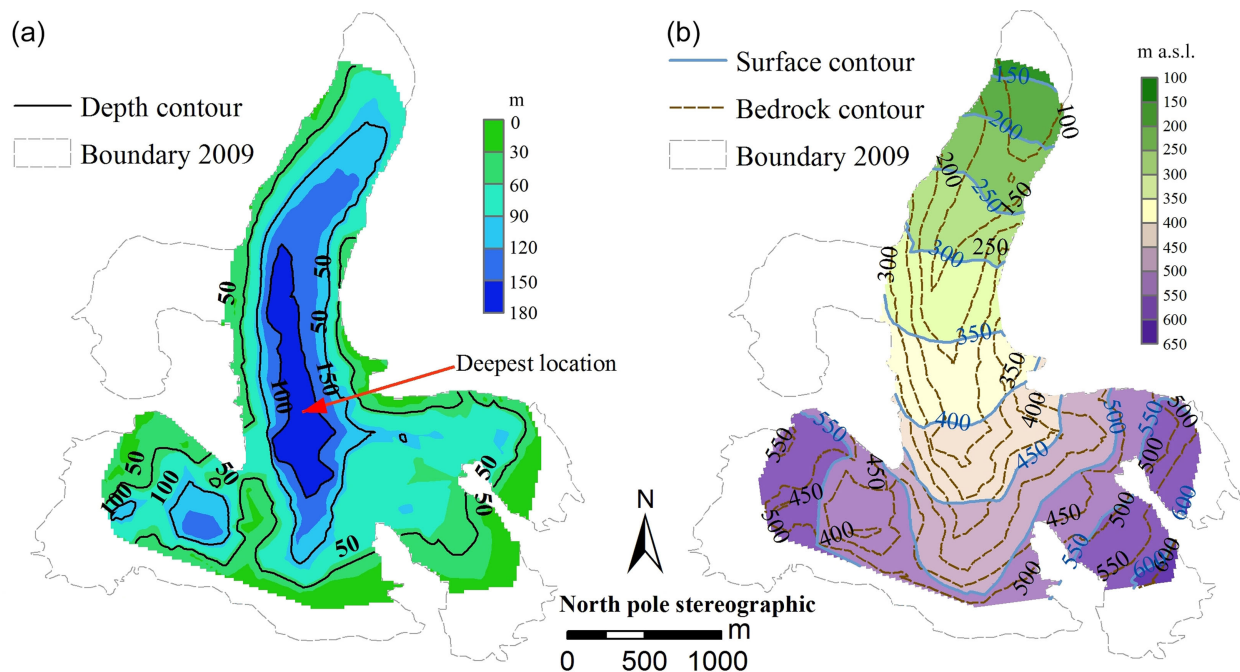


**Fig. 3** (a) Depth/ice thickness distribution on Pedersenbreen. Here, the deepest area presented is under the bottom of the cirque. (b) Surface and bedrock topography for Pedersenbreen, with 50 m intervals between contour lines.

## Results and discussion

Detailed GPR or GPS work has not been performed on Pedersenbreen before now. This paper remedies this deficiency by presenting basic elements of the glacier based on high density field surveying data from GPR & GPS. We present a surface DEM and a bedrock DEM of Pedersenbreen, containing reliable information including surface topography, bedrock topography, ice thickness and ice volume. These basic parameters are useful for future research on glacier mass balance and numerical model simulation.

### Ice thickness and ice volume

Calculated from the surface and bedrock DEM, the ice volume in Pedersenbreen is estimated to be  $0.360 \text{ km}^3$  in the surveyed area, i.e., the surface DEM-covered area (Fig. 3b). According to an empirical formula (Hagen et al. 1993), the mean depth of the north-western tributary is 25 m, so its ice volume is estimated to be  $0.016 \text{ km}^3$ . Similarly, the ice volume of the high-elevation boundary is estimated to be  $0.011 \text{ km}^3$  assuming that the mean depth is 10 m here. The ice volume of unsurveyed tongue area is estimated to be  $0.006 \text{ km}^3$  with portable GPS point data for ensuring front boundary. Over the unsurveyed area, there is an uncertainty of  $\pm 0.015 \text{ km}^3$  given 30% error in unsurveyed tongue volume estimation and

50% error in unsurveyed tributary and boundary areas. Simultaneously, there is an uncertainty of  $\pm 0.022 \text{ km}^3$  for the surveyed area, considering a depth RMSE of 4.6 m and the Kriging interpolation covariance of 0.4 m. There is also another 3% error, about  $0.010 \text{ km}^3$ , considering the RWV difference of 0.005 m/ns. The resulting total ice volume of Pedersenbreen was estimated to be  $0.393 \pm 0.047 \text{ km}^3$  in April 2009.

The maximum depth in Pedersenbreen is estimated to be  $183 \pm 9 \text{ m}$  at its central area. Limited to the surveyed area ( $4.462 \text{ km}^2$ ), the mean ice thickness is 80.7 m. Over the whole glacier, the mean ice thickness is estimated to be 62.0 m, including the uncertain boundary areas and the unsurveyed north-western tributary.

### Bedrock valley feature

We have chosen five different profiles across the surface and bedrock and one along the length of the glacier in Fig. 4 to present the shape of the glacier. These profiles reveal the bedrock valley shape and different correlations between surface and bedrock.

According to the power law model of Svensson (1959), the cross-section data is presented by

$$y = ax^b, \quad (4)$$

where  $x$  and  $y$  are the horizontal and vertical distances from the lowest point of the cross-section, and  $a$  and  $b$

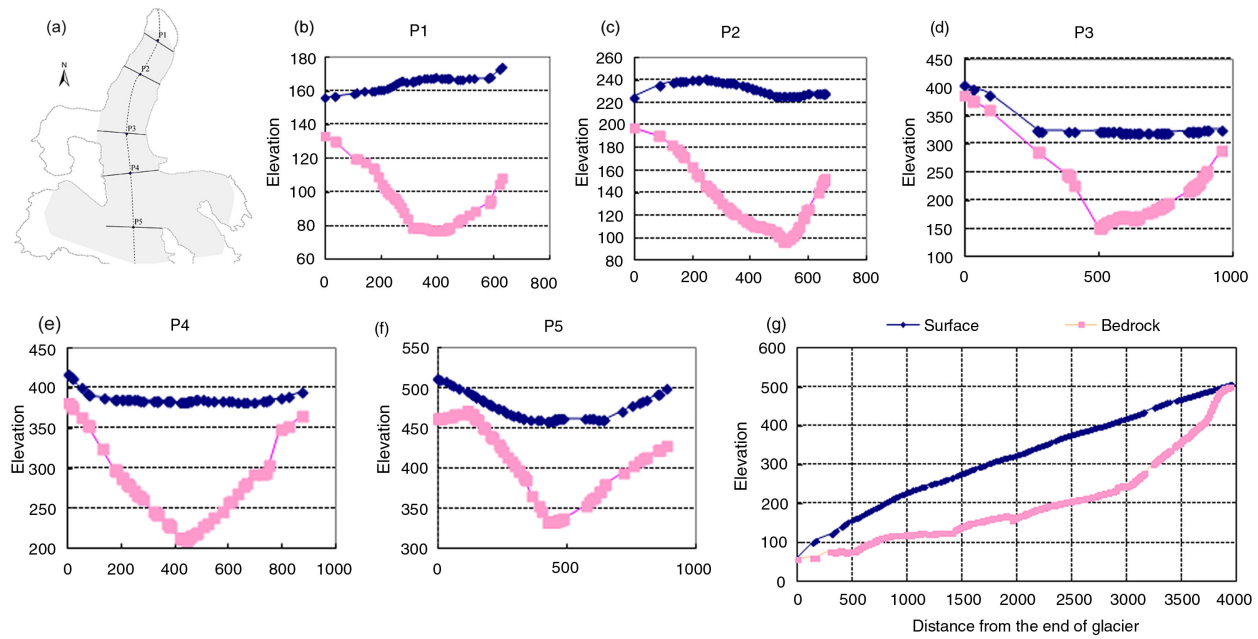


**Fig. 4** Profiles and their positions in Pedersenbreen in April 2009. Profile P3 shows one tributary flowing from the west. Profile P5 shows one tributary flowing from the west, and the bedrock of the tributary has been eroded distinctly. The profile along the central flowline of Pedersenbreen shows that the surface is relatively smooth but the bedrock is irregular.

(commonly used as an index of the steepness of the valley side) are constants. This model has been widely used in the analysis of glacial valley morphology and evolution. Some studies suggested that the valley morphology progressively approaches a true parabolic form with increasing glacial erosion, which can be gauged by the proximity of  $b$  to 2.0 (Svensson 1959; Graf 1970). In the case of Pedersenbreen, the  $b$  values are between 0.71 and 1.89, so the glacier valley of Pedersenbreen is overall V-shaped rather than U-shaped ( $b \geq 2$ ) according to Svensson’s model, which is similar to the valley shape of its neighbouring glaciers, Austre Lovénbreen (Saintenoy et al. 2013) and Midre Lovénbreen (Björnsson et al. 1996). Additionally, in the lower (profiles P1 and P2) and middle (profile P3) glacier, the bed appears to be less eroded in its western part, while there is not a marked difference between both parts in the upper glacier (profiles P4 and P5).

**Surface and volume change**

From a historic topographic map from Norwegian Polar Institute, which shows the surface of Pedersenbreen in 1936, we can compare the surface elevation change between 1936 and 2009. Assuming that the bedrock change is negligible in the past 73 years, the ice volume in the surveying area included in this study is estimated

at  $0.392 \text{ km}^3$  in 1936 using the surface elevation data according to the old map. The ice volume in the retreated tongue area is estimated to be  $0.0316 \text{ km}^3$ , using the currently exposed field as the bed in 1936. Again, we neglect the change in the north-western tributary and the uphill boundary area. Because of the poor quality in the 1936 map, based on aerial oblique photographs, its error in area and volume is difficult to estimate, so we have omitted them, though they are expected to be large. The length along the central line, the area, the ice volume and the mean ice thickness of Pedersenbreen in 1936 and 2009, together with their changes in the period 1936–2009, are shown in Table 3. Just in the retreated tongue area, which only occupied 5% of the whole area in 1936, the lost mass is contributing ca. 33% of the whole mass loss in the past 73 years.

The only available ice volume data of Pedersenbreen is  $0.46 \text{ km}^3$  in 1977 (Hagen et al. 1993), which is calculated

**Table 3** Comparison in geometric change of Pedersenbreen between 2009 and 1936.

Type	1936	2009	Change
Length (km)	5.18	4.55	-0.63 (12.2%)
Planar Area ( $\text{km}^2$ )	6.48	$6.34 \pm 0.07$	-0.14 (2.2%)
Ice volume ( $\text{km}^3$ )	0.447	$0.393 \pm 0.047$	-0.054 (12.1%)
Mean ice thickness (m)	69.0	62.0	-7.0 (10.1%)

from an empirical formula and is larger than the volume both in 1936 and in 2009. Our study suggests that the 1977 volume data is probably an overestimate since we expect that the volume decreased between 1936 and 2009.

## Conclusions

The following main conclusions can be drawn from our analysis. The GPR survey in 2009 confirms that Pedersenbreen has a polythermal structure, with a layer of temperate ice in the lower part of the central bottom cirque. The glacier valley of Pedersenbreen is V-shaped rather than U-shaped. Pedersenbreen has experienced a considerable retreat since 1936, with estimated loss in ice volume of 0.054 km<sup>3</sup> during the period 1936–2009, which represents a 12.1% drop during this period. The remarkable mass loss of Pedersenbreen is mainly on the tongue area of lower altitude, which contributes ca. 33% to the whole mass loss during the past 73 years.

## Acknowledgements

We are very grateful to the anonymous reviewers whose useful comments significantly improved the clarity and presentation of our results. This work was supported by the Chinese Polar Environment Comprehensive Investigation & Assessment Programmes, the National High Technology Research and Development Program of China (2012AA12A304), the National Natural Science Foundation of China (41076126, 41106163, 41174029, 41176172) and the Chinese Polar Scientific Strategy Project (20080203, 20100103). The authors thank the Chinese Arctic and Antarctic Administration, State Oceanic Administration, for sponsoring the field surveying and research works around Chinese Arctic Yellow River Station. Special thanks go to Roger W. Hagerup and Jack Kohler from the Norwegian Polar Institute for their help finding the historical maps for this area. We also thank to Dr Adrian Fox from the British Antarctic Survey for polishing the English of this paper.

## References

Ai S., Dongchen E., Yan M. & Ren J. 2006. Arctic glacier movement monitoring with GPS method on 2005. *Chinese Journal of Polar Science* 17, 61–68.

Bælum K. & Benn D.I. 2011. Thermal structure and drainage system of a small valley glacier (Tellbreen, Svalbard), investigated by ground penetrating radar. *The Cryosphere* 5, 139–149.

Barthier P.M. & Keller C.P. 1996. Multivariate interpolation to incorporate thematic surface data using inverse distance weighting (IDW). *Computers & Geosciences* 22, 795–799.

Björnsson H., Gjessing Y., Hamran S., Hagen J.O., Liestøl O., Pálsson F. & Erlingsson B. 1996. The thermal regime of sub-polar glaciers mapped by multi-frequency radio-echo sounding. *Journal of Glaciology* 42, 23–32.

Graf W.L. 1970. The geomorphology of the glacial valley cross section. *Arctic and Alpine Research* 2, 303–312.

Hagen J.O., Eiken T., Kohler J. & Melvold K. 2005. Geometry changes on Svalbard glaciers: mass-balance or dynamic response? *Annals of Glaciology* 42, 255–261.

Hagen J.O., Kohler J., Melvold K. & Winther J.-G. 2003. Glaciers in Svalbard: mass balance, runoff and freshwater flux. *Polar Research* 22, 145–159.

Hagen J.O. & Liestøl O. 1990. Long-term glacier mass-balance investigations in Svalbard, 1950–88. *Annals of Glaciology* 14, 102–106.

Hagen J.O., Liestøl O., Roland E. & Jørgensen T. 1993. *Glacier atlas of Svalbard and Jan Mayen. Meddelelser* 129. Oslo: Norwegian Polar Institute.

Hagen J.O. & Sætrang A. 1991. Radio-echo soundings of sub-polar glaciers with low frequency radar. *Polar Research* 9, 99–107.

Hambrey M.J., Murray T., Glasser N.F., Hubbard A., Hubbard B., Stuart G., Hansen S. & Kohler J. 2005. Structure and changing dynamics of a polythermal valley glacier on a centennial timescale: Midre Lovénbreen, Svalbard. *Journal of Geophysical Research—Earth Surface* 110, F01006, doi: 10.1029/2004JF000128.

Kääb A., Lefauconnier B. & Melvold K. 2005. Flow field of Kronebreen, Svalbard, using repeated Landsat 7 and ASTER data. *Annals of Glaciology* 42, 7–13.

Köhler A., Chapuis A., Nuth C., Kohler J. & Weidle C. 2012. Autonomous detection of calving-related seismicity at Kronebreen, Svalbard. *The Cryosphere* 6, 393–406.

Macheret Y.Y. & Zhuravlev A.B. 1982. Radio echo-sounding of Svalbard glaciers. *Journal of Glaciology* 28, 295–314.

Meier M.F. 1984. Contribution of small glaciers to global sea level. *Science* 226, 1419–1422.

Moholdt G., Nuth C., Hagen J.O. & Kohler J. 2010. Recent elevation changes of Svalbard glaciers derived from ICESat laser altimetry. *Remote Sensing of Environment* 114, 2756–2767.

Norwegian Polar Institute 1990. *Kongsfjorden, Svalbard, scale 1:100000, sheet A7*. Tromsø: Norwegian Polar Institute.

Norwegian Polar Institute 2008. *Kongsfjorden, Svalbard, scale 1:100000, sheet A7*. Tromsø: Norwegian Polar Institute.

Oerlemans J. & Fortuin J.P.F. 1992. Sensitivity of glaciers and small ice caps to greenhouse warming. *Science* 258, 115–117.

Paterson W.S.B. 1981. *The physics of glaciers*. Oxford: Pergamon Press.

Rolstad C. & Norland R. 2009. Ground-based interferometric radar for velocity and calving-rate measurements of the tidewater glacier at Kronebreen, Svalbard. *Annals of Glaciology* 50, 47–54.

- Saintenoy A., Friedt J.-M., Booth A.D., Tolle F., Bernard E., Laffly D., Marlin C. & Griselin M. 2013. Deriving ice thickness, glacier volume and bedrock morphology of the Austre Lovénbreen (Svalbard) using ground-penetrating radar. *Near Surface Geophysics* 11, 253–261.
- Smith B.M. & Evans S. 1972. Radio echo sounding: absorption and scattering by water inclusion and ice lenses. *Journal of Glaciology* 11, 133–146.
- Svensson H. 1959. Is the cross-section of a glacial valley a parabola? *Journal of Glaciology* 3, 362–363.
- Xu M., Yan M., Ren J., Ai S., Kang J. & Dongchen E. 2010. Surface mass balance and ice flow of the glaciers Austre Lovénbreen and Pedersenbreen, Svalbard, Arctic. *Chinese Journal of Polar Science* 21, 147–159.